Fusion Engineering and Design 209 (2024) 114698

Contents lists available at ScienceDirect

Fusion Engineering and Design

journal homepage: www.elsevier.com/locate/fusengdes

Numerical structural analysis and flow-induced vibration study in support of the design of the EU-DEMO once-through steam generator mock-up for the STEAM experimental facility

I. Catanzaro [a,*], G. Bongiovì [a], S. Giambrone [a], A. Gioè [a], P. Arena [b], A. Del Nevo [b], M. Eboli [b], S. Basile [a], R. Burlon [a], P. Chiovaro [a], P.A. Di Maio [a], M. Giardina [a], A. Quartararo [a], E. Tomarchio [a], E. Vallone [a]

[a] Department of Engineering, University of Palermo, Viale delle Scienze, Ed. 6, 90128, Palermo, Italy
[b] Nuclear Department, ENEA C. R. Brasimone, 40032, Camugnano, (Bologna), Italy

ARTICLE INFO

Keywords:
DEMO PHTS
OTSG
Vibrations
Pipe stress analysis
3D FEM analysis

ABSTRACT

ENEA, as part of the EUROfusion consortium, is working at the realization of STEAM, an experimental facility integrated into the Water-cooled lithium lead-thermal-HYDRAulic (W-HYDRA) platform, envisaged for the qualification of the EU-DEMO steam generator during the different operational phases of a fusion reactor. It will aim at testing and qualifying the technological solutions to be adopted for the Primary Heat Transport System (PHTS) of the Water-Cooled Lead Lithium Breeding Blanket (WCLL BB). In particular, a mock-up of the Once-Through Steam Generator (OTSG) foreseen for the PHTS of the DEMO WCLL BB will be designed, installed and tested within STEAM. In this regard, a campaign of numerical structural analyses and a preliminary flow-induced vibration study have been carried out at the University of Palermo, in close collaboration with ENEA Brasimone. Firstly, a pipe stress analysis has been conducted focussing on the structural performances of the surge line devoted to connecting the STEAM facility to the pressurizer, looking at the stress and displacement arising under the nominal operating conditions so to propose proper design modifications. Secondly, in order to investigate the structural performances of the DEMO OTSG mock-up in the envisaged nominal operating scenario, a 3D steady-state thermo-mechanical FEM analysis has been carried out. The outcomes have allowed selecting the most critical regions in view of the adopted structural design code. Lastly, in order to preliminarily assess the potential onset of vibration-induced issues within the tubes of the DEMO OTSG mock-up, a preliminary analytical study has been carried out adopting formulae available in literature. The scope has been to establish if vibration-induced issues in the tubes can be reasonably excluded or if they could represent a tangible concern, to be further assessed. Models, assumptions and outcomes are provided and critically discussed.

1. Introduction

The Water thermal-HYDRAulic (W-HYDRA) experimental platform, set up at ENEA-Brasimone Research Center, is intended to support the research and development activities on the DEMO Water-Cooled Lead Lithium (WCLL) Breeding Blanket (BB) [1,2], acting as a test rig for the experimental validation of its thermal-hydraulic behaviour. Hence, W-HYDRA will permit to instal mock-ups of the most relevant DEMO components (such as, but not limited to, first wall and manifolds) to be tested under different loading conditions in order to collect data coming from experimental tests, allowing benchmarking the numerical models adopted so far and proving the effectiveness of the envisaged design solutions. In this way, experimental outcomes can be gathered in support of the selection of the driver blanket concept for DEMO, expected at the end of the Conceptual design phase. Specifically, the STEAM facility is one of the three experimental facilities composing the W-HYDRA platform, aimed at investigating the WCLL BB Primary Heat Transfer System (PHTS) components, whose primary function is to extract power from the BB and transfer it to the Balance of Plant (BoP) system for the conversion into electricity. In particular, the STEAM facility houses a mock-up of the Once-Through Steam Generator (OTSG) envisaged for the WCLL BB PHTS.

* Corresponding authors.
E-mail address: ilenia.catanzaro@unipa.it (I. Catanzaro).

https://doi.org/10.1016/j.fusengdes.2024.114698
Received 1 August 2024; Received in revised form 25 September 2024; Accepted 19 October 2024
Available online 31 October 2024

In this context, the University of Palermo has been involved in the design of the STEAM facility and of the OTSG mock-up. In particular, the pipe stress analysis of the STEAM facility loop (reported in Section 2), the 3D structural analysis of the OTSG mock-up (reported in Section 3) and the preliminary study of the tube vibrations in the OTSG mock-up (reported in Section 4) have been conducted and presented in this paper.

To this purpose, the 1D Finite Element method (FEM) code ROHR2 has been adopted for pipe stress analysis, whereas the 3D FEM code Ansys Mechanical has been used for the OTSG mock-up thermo-mechanical analysis. Lastly, a verification by formula approach has been adopted for the preliminary analysis of the tube vibrations in the OTSG mock-up.

2. Pipe stress analysis of the STEAM facility

In order to contribute to the design of the STEAM facility, a campaign of pipe stress analysis has been launched focussing on the structural performances of the pressurizer surge line, that STEAM shares with another facility composing the W-HYDRA platform (i.e. the Water Loop facility, Fig. 1). A comprehensive geometric model has been considered and a proper FEM model has been built to perform the analysis campaign [3] but, for the sake of brevity, only modelling and results concerning the pressurizer surge line are here reported and discussed. The chosen loading scenario has been established according on the equivalent scenario selected for the ITER WCLL-TBM WCS [4], namely the Plasma/Normal Operation State (POS/NOS) loading conditions, classified as Category I in view of the code&standards. The study has been carried out using the commercial code ROHR2 v33 [5]. The ASME BPVC Sect. III [6] standard (release 2019), implemented in ROHR2 libraries, has been considered for the piping structural assessment. In particular, since the circuit has been considered as Class 2 component the ASME BPVC Sect. III Class 2 has been adopted.

The AISI 316L steel has been considered as the structural material for the STEAM surge line. A NSP2, schedule 160 pipe, covered by 40 mm of PAROC mineral wool (characterized by a density of 80 kg/m^3) as thermal insulator has been selected for the assessed surge line. The temperature-dependent material properties have been directly called from the ROHR2 material library.

Once assigned the supports to the whole assessed loop and defined the interfaces and the connections with other systems and components by means of proper mechanical restraints, loads have been assigned. As reported in Fig. 1, combination of rigid hangers and rigid supports have been used for the support scheme of the whole system. Moreover, the interface with the pressurizer has been simulated defining a proper nozzle, "pressurizer connection" in Fig. 1. In fact, in order to simulate the connection with the pressurizer, in ROHR2 it is possible to assign a certain flexibility to the nozzle by means of a spring element, that is a flexible element whose elastic behaviour is calculated by the code by providing the geometric characteristics of the component it is connected to (height, diameter and thickness). For each component located within the circuit, for example filters and valves, the weight has been specified, in order to take it into account as part of the global dead load that affects the system. Moreover, a pressure load of 154.8 bar and a temperature of 327.4 °C has been supposed holding within the surge line piping.

Once defined the model, the analysis has been run. The assessment of the results considers different load combinations, each one characterised by a relevant structural criterion, as follows:

- Primary Loads or Sustained Loads (SSL): primary loads (i.e. dead weight and internal pressure);
- Secondary Loads or Thermal Range (SE): axial thermal expansion;
- Primary plus Secondary Loads (STE): all the loads occurring during the normal operation loading scenario.

In order to evaluate the structural performances of the system, the "Utilization Factor" UF, that is calculated as the percentage ratio between the equivalent stress (σ_{eq}) and the allowable stress (σ_{all}), has been considered. In particular, σ_{eq} is the equivalent stress acting on the section under investigation, typically defined combination of primary and/or secondary stress on the basis of the selected design criteria, and σ_{all} represents the temperature-dependent maximum allowable stress defined by the design criteria, that usually depends on the yield or ultimate strength of the material. The considered criterion is not verified in the examined region when the UF exceeds 100%. The analysis carried out has shown that the effect of SSL only is not critical at all since the resulting displacement remains below 3 mm and the UF is largely lower than 30 %. These results are not shown for brevity's sake. Concerning SE and STE, the results obtained in terms of displacements and utilization factors are reported in Fig. 2. In particular, Fig. 2 the deformed vs. undeformed shape with an amplification factor equal to 20, the displacement field and the Von Mises equivalent stress field for total loads and the UF contour maps for SE and STE loads are reported.

As it can be observed, displacement under total loads achieves reasonable values (less than 25 mm). so it can be considered acceptable. Instead, the structural design criteria are not totally verified and design modifications need to be introduced with the aim of allowing the whole system safely withstanding the loading conditions.

Considering that the high UF values are mainly attributable to the high operating temperature and the proximity with a vessel junction (SE-PRZ-003 in Fig. 1), the horizontal segment of the red pipe has been

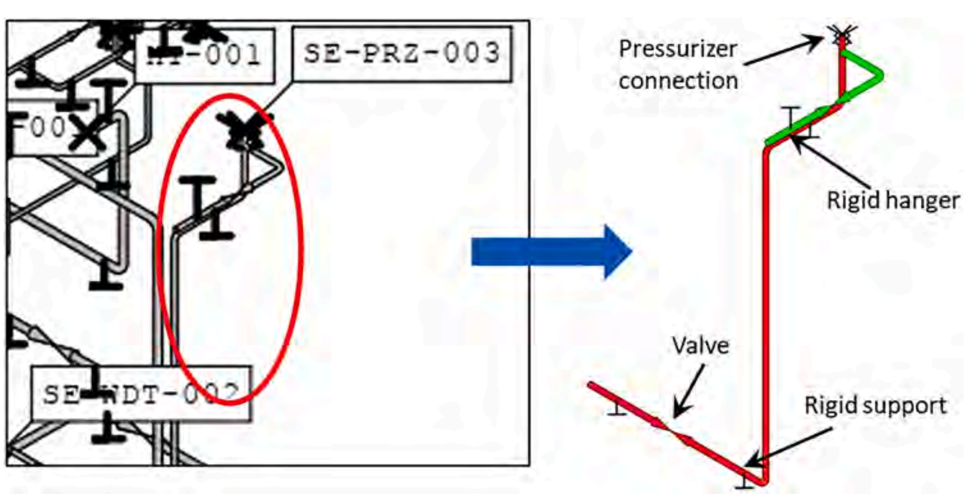

Fig. 1. STEAM-Water Loop pressurizer surge line modelled within the ROHR2 code.

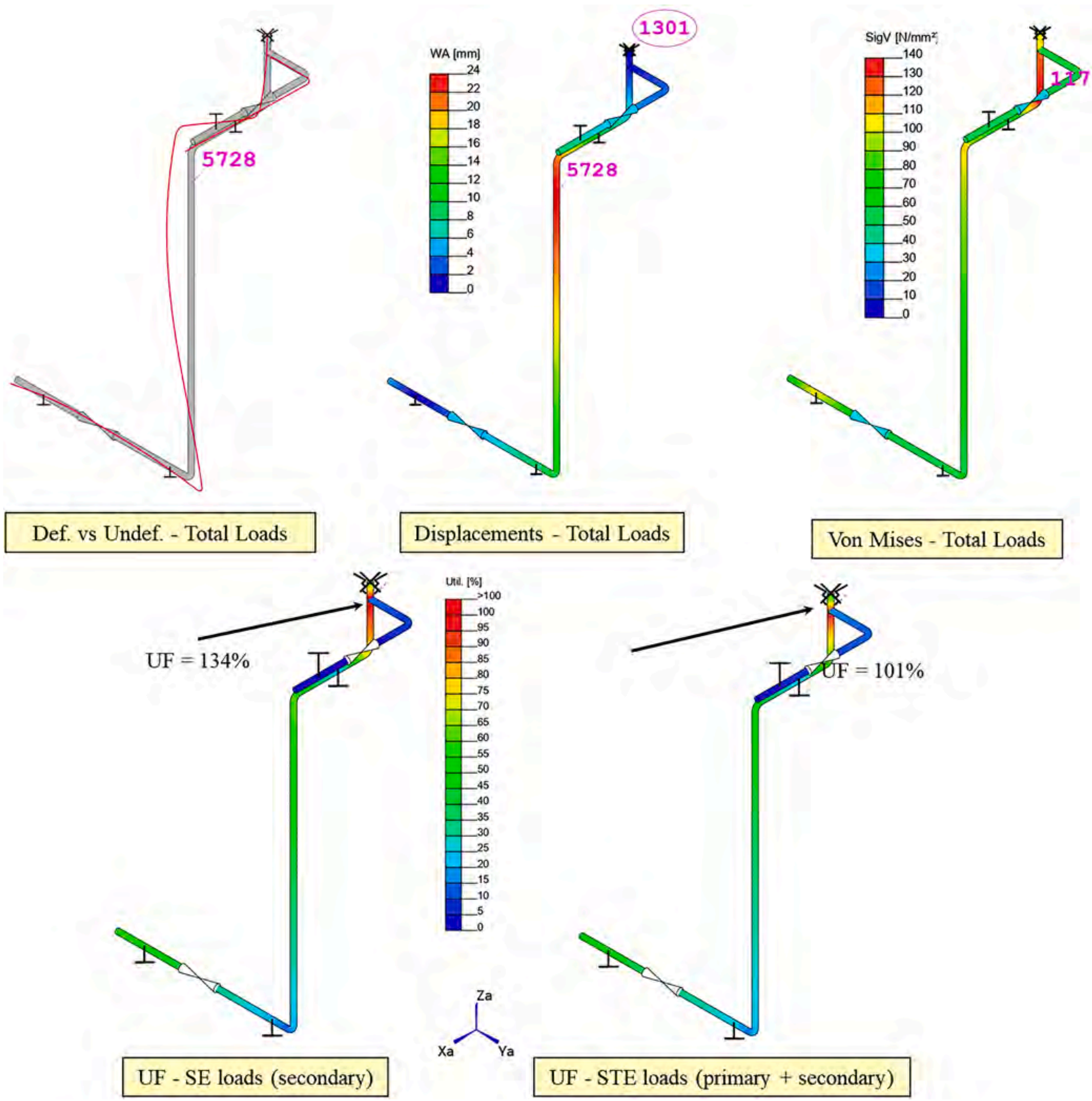

Fig. 2. Results under POS/NOS Cat. I loading scenario.

moved vertically by 700 mm (Fig. 3), in order to reduce that UF values and avoiding failure in the criteria verifications. Hence, the model has been consequently edited and a new analysis has been run. As depicted in Fig. 4, the proposed piping modification allows reducing the UF for SE and STE loads well below the limit of 100% in the whole assessed domain.

In conclusion, the performed pipe stress analysis of the STEAM facility's pressurizer surge line has allowed improving its original design, finding a geometric layout able of totally fulfilling the prescribed structural design criteria ensuring reasonable displacement.

3. The structural analysis of the OTSG mock-up

3D steady-state thermal and structural analysis of the DEMO OTSG mock-up during the nominal operating loading scenario have been conducted to preliminary assess its structural behaviour. To this purpose, the provided geometric model has been adopted assuming a proper set of boundary conditions to simulate the support system and the continuity of the piping. A 3D FEM model has been set up and the steady-state structural analysis has been performed using the Ansys Steady State Thermal and the Ansys Mechanical modules of the Ansys Workbench calculation suite. The geometric layout of the OTSG mock-up is shown in Fig. 5. The OTSG is a shell-and-tube vertically oriented heat exchanger, once-through, up boiling and cross-counter-flow. The primary coolant enters from the top, goes down through the tubes and exits at the lower part. The feedwater (namely the secondary fluid) enters through a nozzle positioned slightly above the centre of the OTSG, mixing with the steam spilled from the secondary fluid recirculation pipe and it is injected in the bottom part of the OTSG. Then, it moves upward exiting from the secondary fluid outlet pipe, showed in Fig. 5.

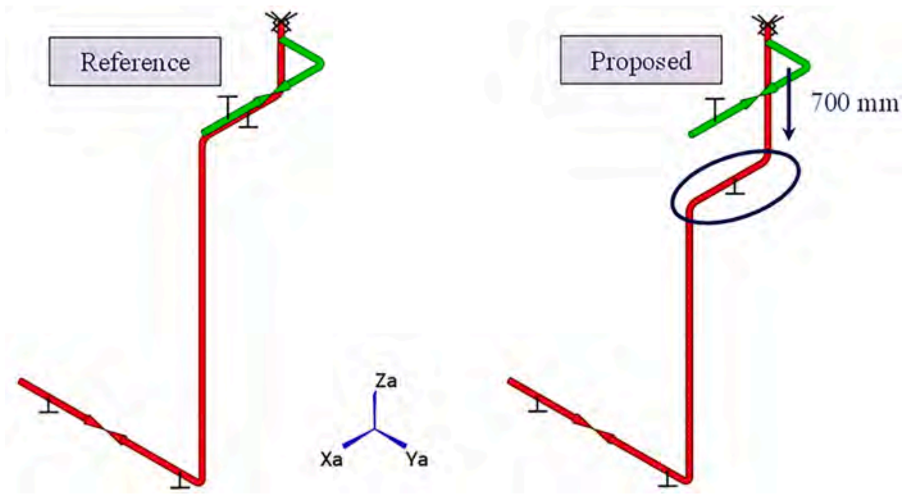

Fig. 3. STEAM surge line design modification.

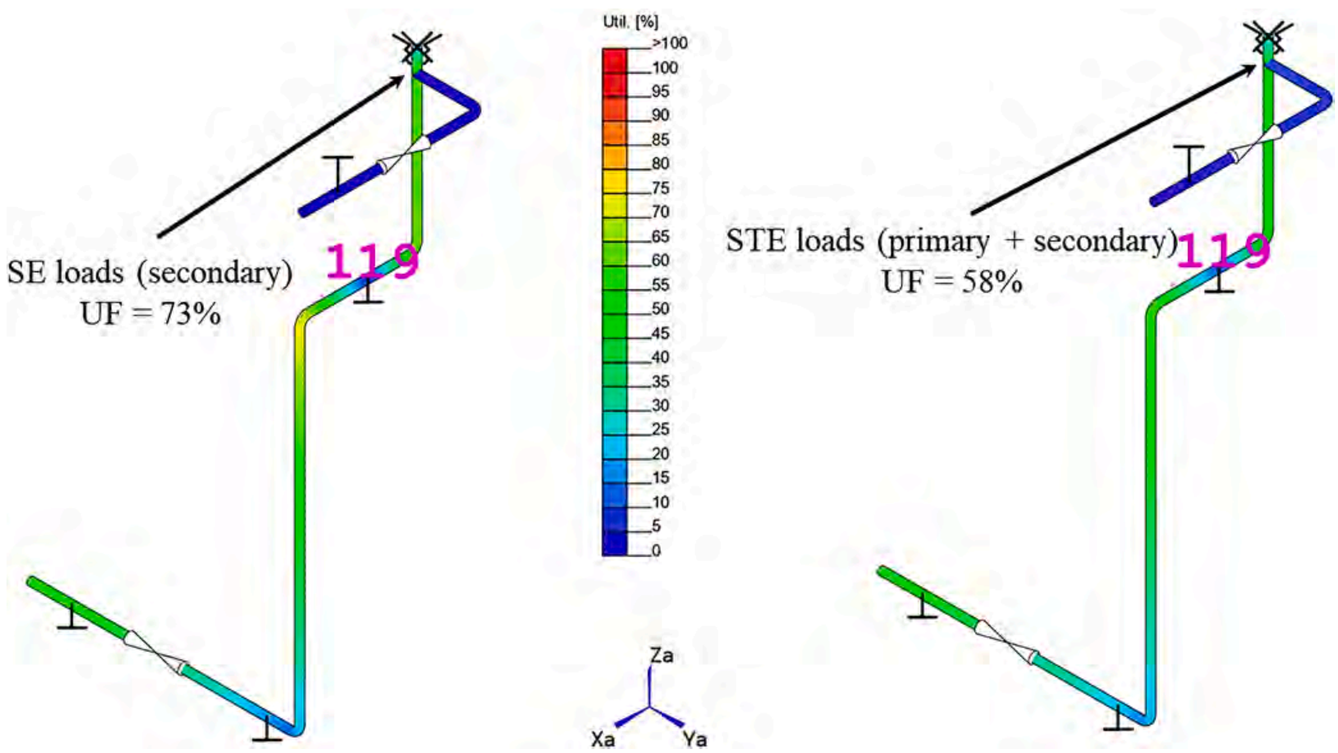

Fig. 4. UF contour maps for the modified surge line geometry.

Moreover, a section view of the OTSG is reported in Fig. 5 where the 37 tubes of the tube buddle can be observed. The tubes are considered tied to the bottom and upper tube-sheets and moreover, a series of baffle plates are located at different heights of the OTSG, in order to ensure the right positioning of the tubes during the operation. In particular, it can be noticed that baffle plates holes diameter is greater than the tube external one, namely no contact is foreseen by design.

3.1. The FEM model

Adopting the previously depicted geometric model, a mesh consisting of approximately 3M tetrahedral and hexahedral elements of both first and second order, connected in approximately 2M nodes, was generated. The materials chosen for the characterization of the model, assumed having temperature-dependent properties, are INCONEL alloy 690 (UNS N06690/W. No. 2.4642) [7] for the heat exchanger tubes, and AISI 316L [8] for the rest of the structure. It should also be noted that in the mechanical analysis, to consider the presence of water inside the exchanger and therefore its weight, the density of the AISI 316L has been properly modified adopting an equivalent density, calculated considering the total amount of water and steel and the corresponding density, functions of the temperature.

3.2. The thermal analysis

To perform the 3D thermal analysis, on the basis of data reported in [9] and shown in Fig. 6, temperature profiles were assigned to the model surfaces as Dirichlet-type boundary conditions.

First, the temperature profile depicted in blue in Fig. 6 has been assigned to the internal walls of the heat exchanger tubes, to consider

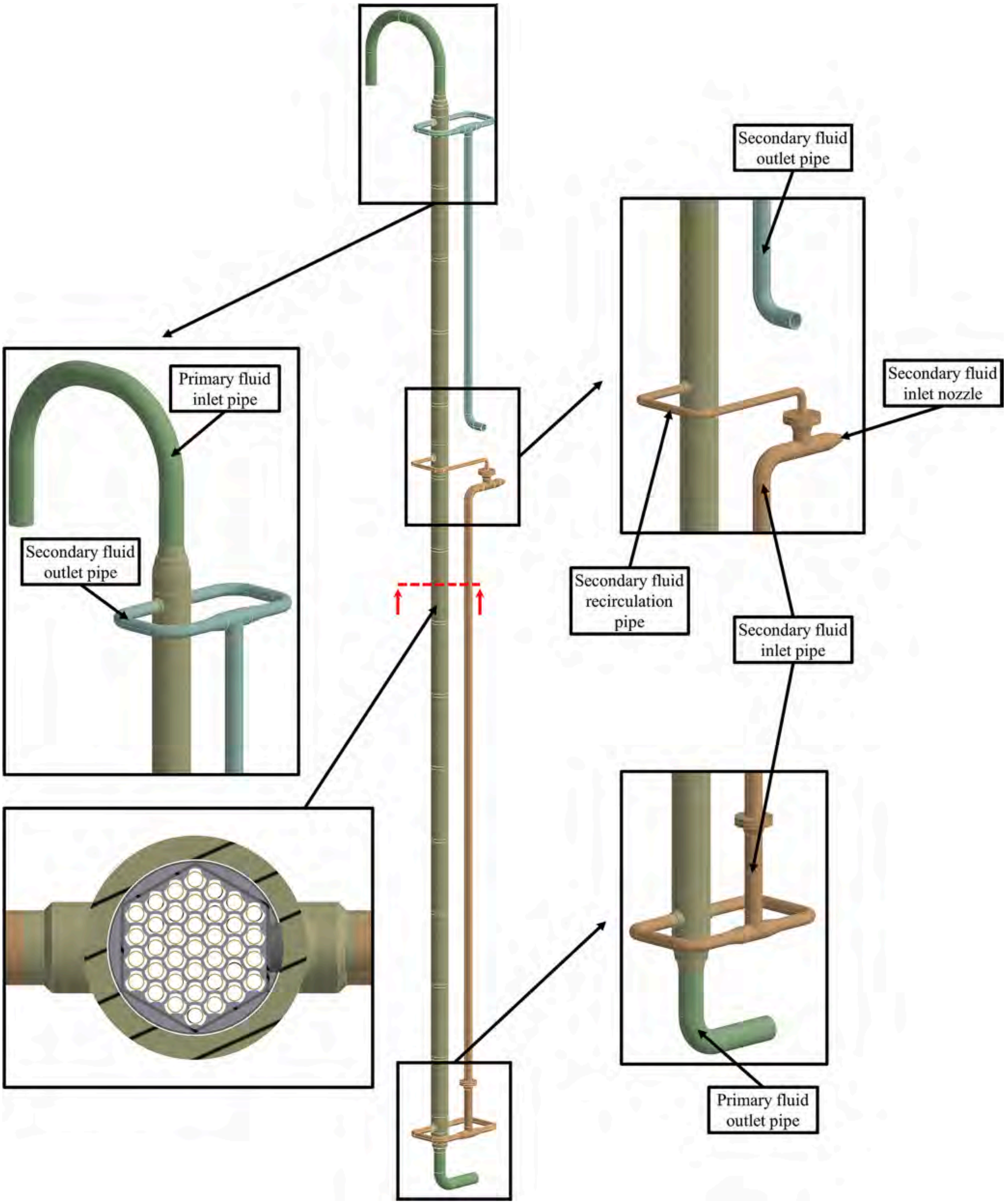

Fig. 5. OTSG mock-up geometric layout.

the thermal action of the primary fluid. On the other hand, the orange temperature profile has been assigned to the external walls of the heat exchanger tubes, wetted by the secondary fluid. Then, the purple temperature profile has been assigned to the internal walls of the heat exchanger cylindrical shell. Lastly, the green temperature profile has been assigned to the tube plates and to the hexagonal shroud.

A temperature of 280 °C has been assigned to the internal walls of the inlet and recirculation piping of the secondary fluid. Moreover, a temperature of 229.1 °C (subcooled liquid) has been assigned to the inlet nozzle of the secondary fluid (Fig. 5), whereas a temperature of 313 °C has been imposed to the secondary fluid outlet pipe internal surfaces. As to the primary fluid piping a temperature of 327.53 °C has been imposed

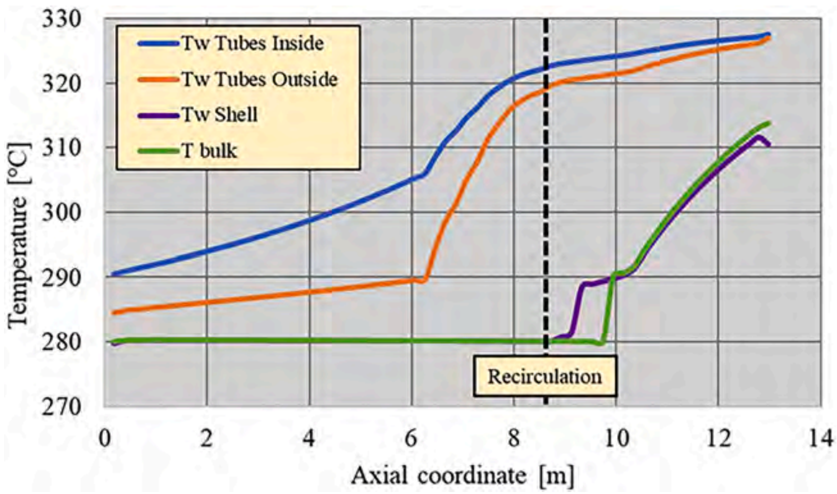

Fig. 6. Temperature profiles assumed as Dirichlet-type boundary conditions.

to the primary fluid inlet pipe internal surfaces whereas a temperature of 290.52 °C has been imposed to its outlet pipe internal surfaces (see Fig. 5). Lastly, all the other surfaces in the model were considered adiabatic.

As a result, the temperature field calculated within the shell and the external piping together with the thermal field obtained within the internal tubes are depicted in Fig. 7.

3.3. *The thermo-mechanical analysis*

To study the structural behaviour of the OTSG mock-up under nominal operating conditions, a steady-state mechanical analysis was carried out. In particular, besides considering the thermal load obtained from the previous thermal analysis, a pressure value of 15.5 MPa has been imposed on all surfaces wetted by the primary fluid. Moreover, a pressure of 6.4 MPa has been imposed onto all surfaces wetted by the secondary fluid. The gravity load was also considered, as already mentioned.

Regarding the contacts in between tubes and plates, a bonded contact model has been imposed between tubes and tube-sheets holes surfaces. Moreover, proper contact models were set up, with a 0.7 friction coefficient between tubes and baffle plates holes. Indeed, although the baffle plates and tubes are not in contact by design, contacts may occur because of the relative deformation and then the implemented contact models allow to take into account the exchanged contact forces, if any.

With the aim of simulating the presence of a support system for the heat exchanger mock-up as well as the continuity of the external piping, a suitable set of boundary conditions has been selected (Fig. 8).

Once the analysis was carried out, the most critical areas in terms of stress have been identified. The criterion used for their identification was to calculate the ratio between the equivalent Von Mises stress (VM) and the stress limit value associated with each material [10]. When the ratio is greater than one, it will therefore mean that, at that point, the equivalent stress is higher than the stress limit value at that given temperature. This procedure allows to identify areas that would otherwise be difficult to highlight because they are apparently not too much stressed only looking at the Von Mises stress field (Fig. 7). On this basis, two areas were taken into consideration on the structure of the heat exchanger shell and one area on the tubes, and a total of four paths (S_1, S_2, S_3 and T_1) were selected, as shown in Fig. 9 and Fig. 10, in order to perform the stress linearization procedure.

A proper set of rules taken from ASME [11] code was chosen to evaluate the structural integrity of the component: $P_m \leq S$, $(P_m+P_b) \leq 1.5\bullet S$, $(P+Q+F) \leq 3\bullet S$, $P_m \leq 1.2\bullet S$. After a stress linearization procedure, the results were compared to the stress limits taken from the ASME code and are shown in Fig. 11. These results show that structural integrity is ensured throughout most of the model. However, a couple of areas are worthy of attention. Specifically, they are the connection area between the primary fluid inlet pipe and the heat exchanger (path S_1) and that within the thickness of the secondary fluid inlet pipe at the recirculation height (path S_3). In the first case, it may be necessary to carry out pipe stress analyses in order to obtain more realistic boundary conditions, while in the second case, the pipe results undersized in terms of thickness because the criteria taking into account primary loads are not verified.

Lastly, it should be noted that other critical zones were found at the contact areas between the tubes and tube plates. However, no path was built at these points as they are heavily influenced by the formulation chosen for the contacts. Indeed, the predicted high stress is surely overestimated because of the adoption of the contact model.

In order to explore possible solutions to overcome the criticality emerged in the recirculation pipe (i.e. path S_3), a further analysis with an additional constraint has been performed rather than simply increasing the pipe thickness. Indeed, an asymmetry in the recirculation pipe displacement field, caused by the forces exerted onto the pipe because of the mock-up body deformation, can be noted. Hence, the displacement along the X direction has been prevented to the nodes highlighted in Fig. 12 in order to simulate a further support localized in this region.

The obtained results show that values around 0.2 are obtained for the criteria in the recirculation pipe region, significantly lower than in the previous case where the calculated VM was remarkably greater than the stress limit. Hence, one can conclude that the introduction of the new restraint generates a significant reduction of the stress amount in the recirculation pipe region, giving a considerable margin for the fulfilment of the considered structural design criteria.

4. Study of the tube vibrations in the OTSG mock-up

The aim of the study reported in the present section is to carry out a preliminary assessment of the possibly arising vibration-induced problems within some tubes considered particularly critical in the DEMO OTSG mock-up, by following the procedure [12]. It is important to emphasise that the methods and equations typically adopted in vibration studies have considerable margins of uncertainty, because they do not consider all the phenomena that could cause vibrations (some of which are stochastic in nature) and because they are highly reliant on parameters of the tube lattice. In any case, the scope of the assessment is to give helpful insights in order to determine whether problems induced by vibration in the pipelines can be totally excluded (which can be

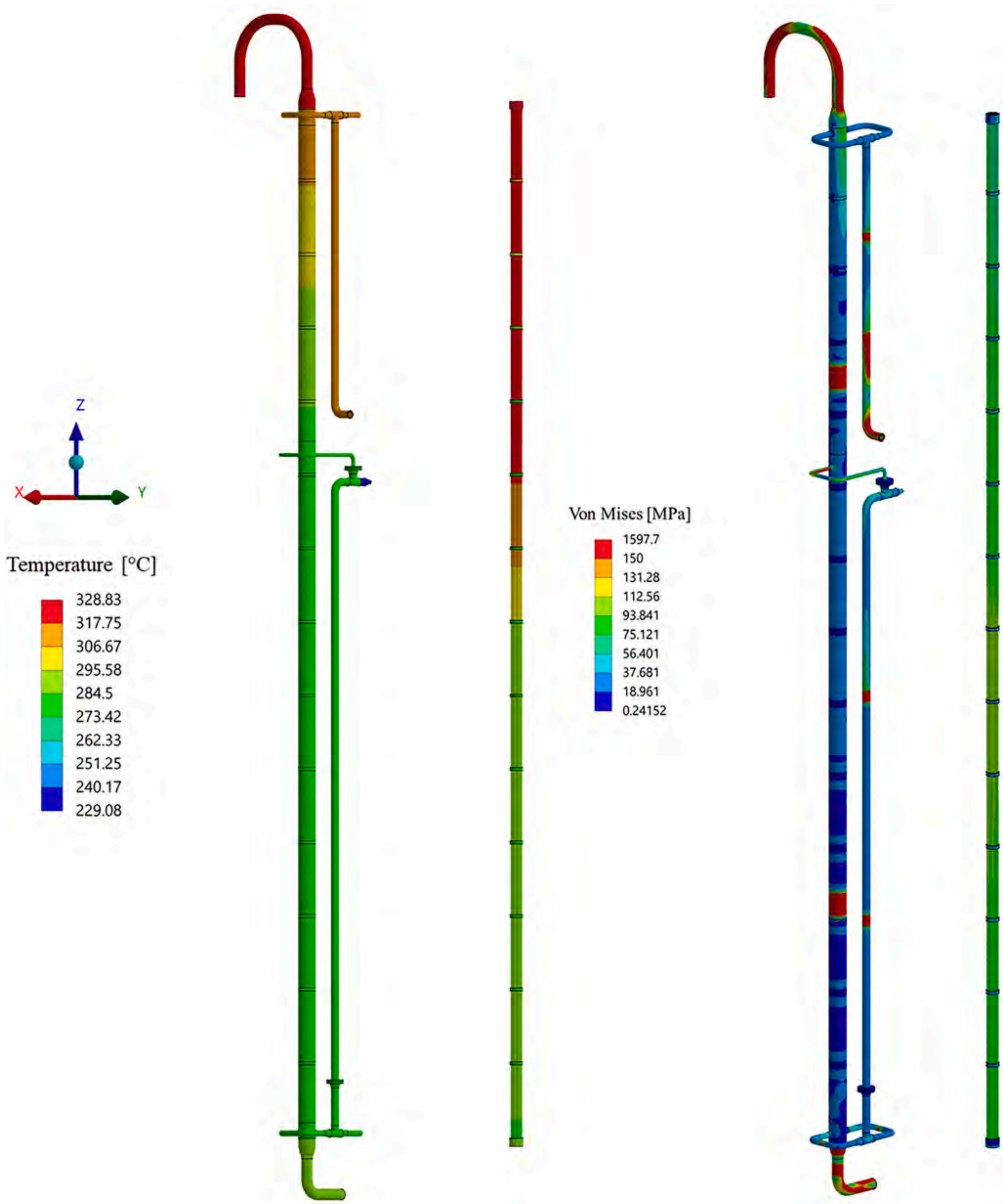

Fig. 7. Temperature and Equivalent Von Mises stress field.

affirmed when the criteria are verified by wide margins) or whether they may be concrete issue, necessitating a more in-depth study.

4.1. The adopted methodology

With regard to the preliminary study of the vibration-induced issues on the OTSG mock-up, three regions have been selected: (i) the secondary fluid inlet section, located at the lower part, (ii) in correspondence of Z = 8.722 (approximately around the middle of the mock-up), and (iii) the secondary fluid outlet section, in the upper part of the mock-up (Fig. 5). In (i) the incoming fluid is in the saturated liquid condition, in (ii) the secondary fluid is considered as saturated steam and, finally,

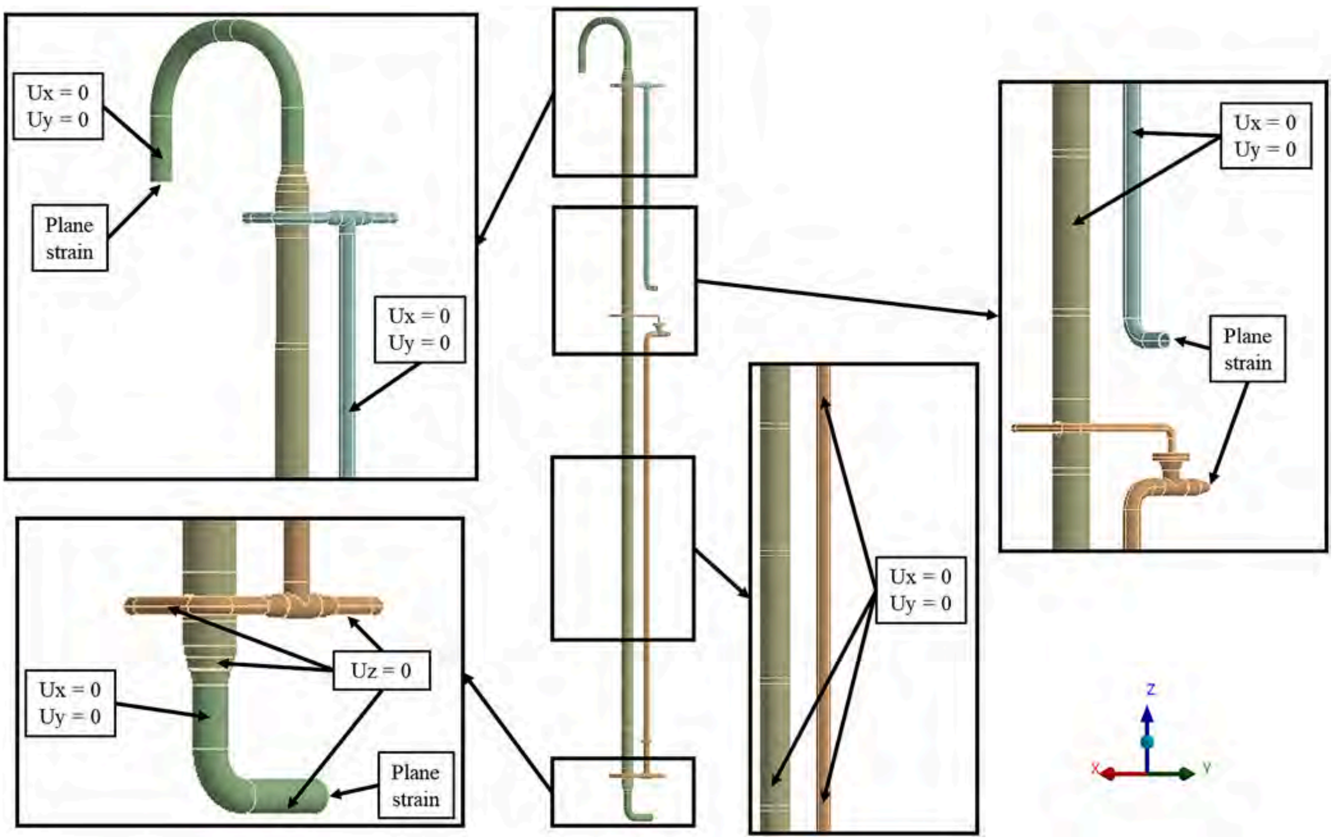

Fig. 8. Location of the boundary conditions.

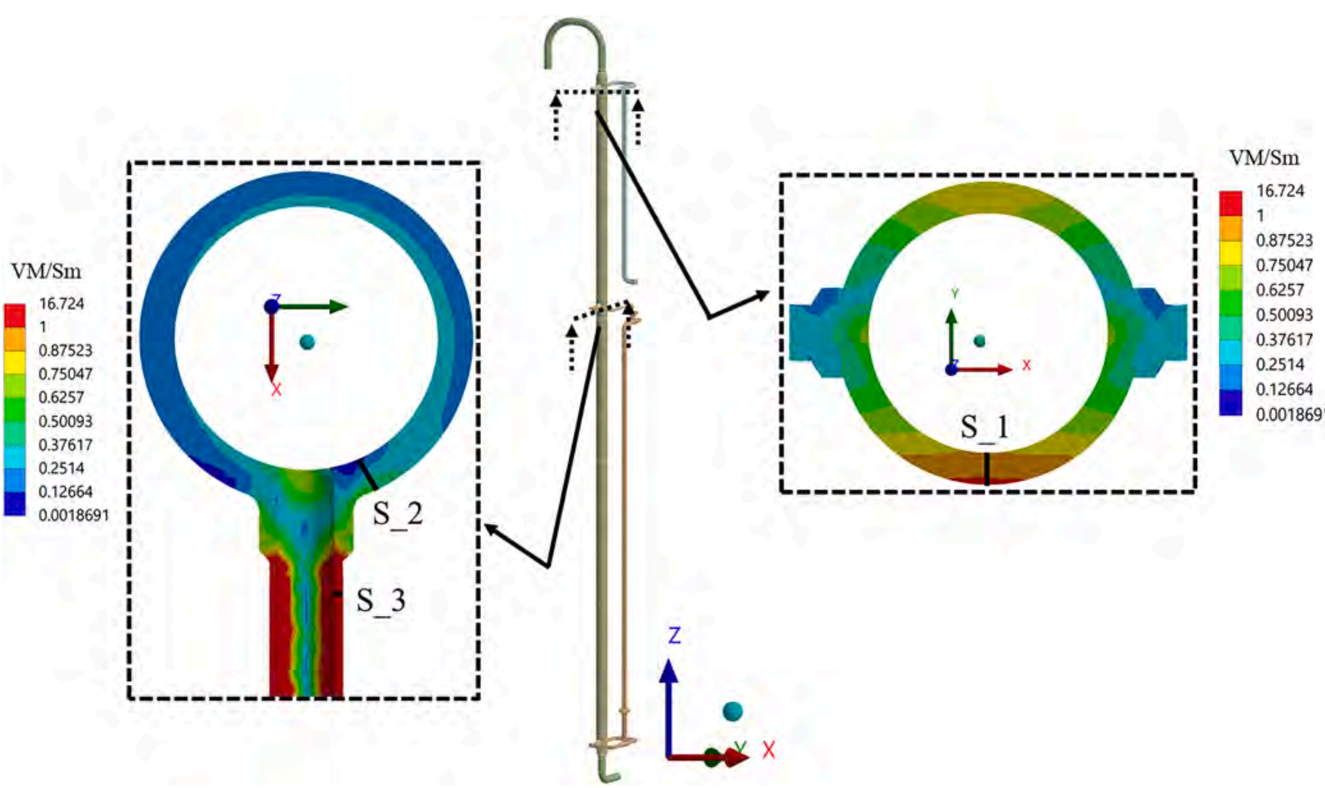

Fig. 9. VM/S_m field and paths S_1, S_2 and S_3 selected on heat exchanger shell.

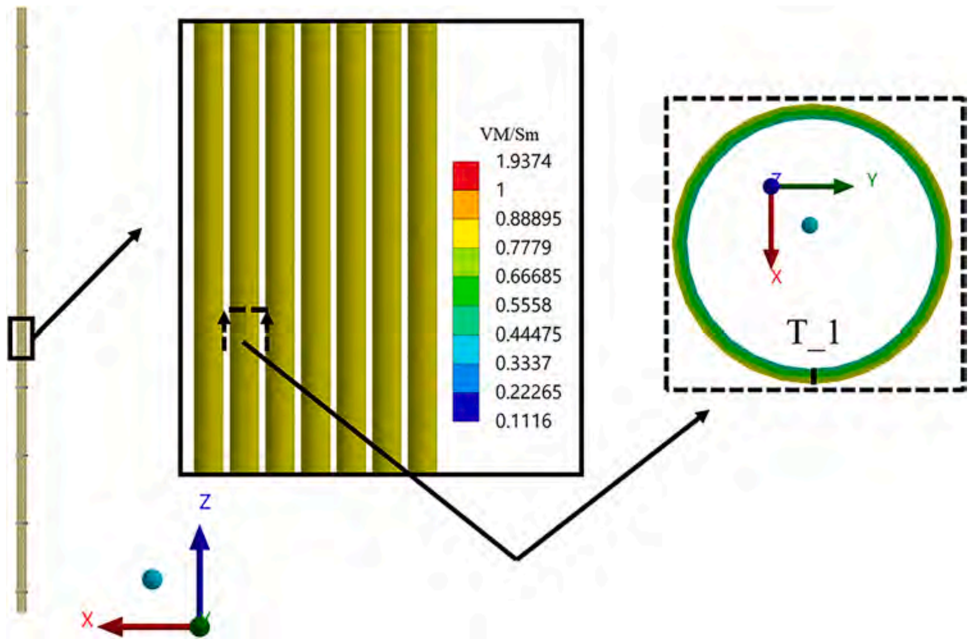

Fig. 10. VM/S_m field and path T_1 selected on the tubes.

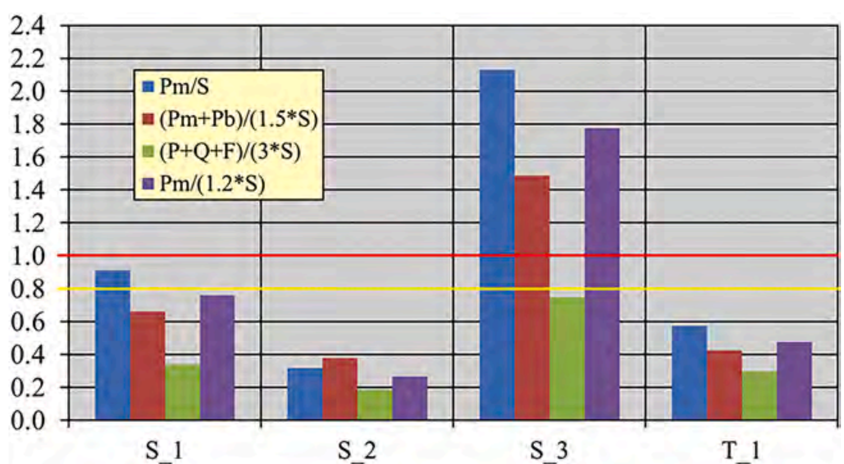

Fig. 11. Structural criteria verification.

in (iii) the exiting fluid is in the superheated steam condition.

These sections have been considered as critical within the OTSG mock-up and it is reasonable to assume that significant vibrations can arise. In particular, in each of the three regions, the vibrations that could be caused by the parallel flow have been examined. Moreover, within section (i) the fluid stability check and the wake shedding one have been conducted. Then, within sections (ii) and (iii), in which steam is present, fluid elastic stability, acoustic vibration and random excitation study have been carried out. For the sake of brevity, the entire study, including all the formulas and calculations, of the secondary fluid outlet section only is herein reported. In any case, the whole study using the same equations can be carried out for the other sections, with the appropriate modifications if the fluid is in saturated liquid, saturated steam or superheated steam condition. A summary of the results obtained within these two sections is given at the end of the present chapter.

In order to perform the vibration assessment, the input data and the geometric parameters reported in Table 1 and Table 2 have been used, taken from [13] and [10], or obtained from basic geometric calculations on the basis of the provided input and geometric parameters.

4.2. *Analysis and results*

As a first step, the tube section moment of inertia I has been calculated equal to 1.151E-09 m^4. For the three sections considered in the study, the single span tube approach has been adopted and then the data reported in Table 3 has been considered.

4.2.1. *Secondary fluid outlet section*

The secondary fluid outlet section – primary fluid inlet section, considered for the assessment of the flow induced tube vibrations, is located at the highest Z coordinate. The secondary fluid has been considered as superheated steam and, therefore, the fluid elastic stability check, the acoustic vibration check and the random excitation check have been carried out, together with the assessment of the vibrations due to parallel flow. Since the considered section presents a double inlet, the section area A equal to 0.005468 m^2 can be obtained as:

$$A = 2\pi \frac{S_d^2}{4} \tag{Eq. 1}$$

On this basis, the cross-flow velocity, v = 10.43 m/s, has can be

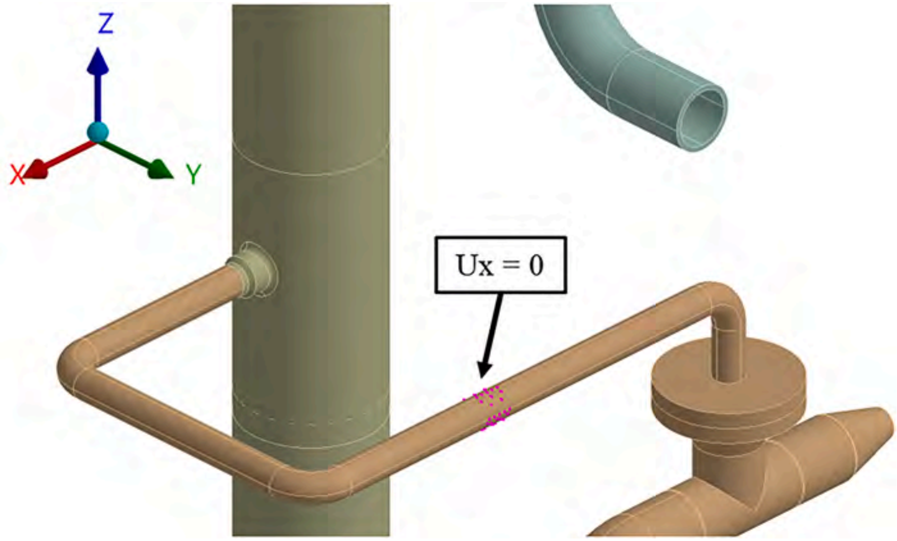

Fig. 12. Added constraint to the recirculation pipe.

Table 1
Input data.

Tube outer diameter, d_o [m]	1.59E-02
Tube inner diameter, d_i [m]	1.41E-02
Layout angle [°]	60
Tube layout pitch, p [m]	0.02
p / d_o	1.4
Secondary fluid mass flow, G [kg/s]	1.63
Secondary fluid pressure [bar]	64.1
Primary fluid pressure [bar]	155
Secondary fluid saturation temperature [°C]	279.93
Primary fluid saturation temperature [°C]	344.79
Tube metal density, ρ_m [kg/m^3]	8340
Young's Modulus of the tube material, E [Pa]	2.07E+11
Maximum allowable stress of the tube material, S_m [Pa]	1.61E+08
Recirculated mass flow rate, G_{rec} [kg/s]	2.27E-01

Table 2
Geometric parameters.

Shroud perimeter [m]	0.48
Tube section moment of inertia I [m^4]	1.15E-09
Shroud cross section [m^2]	1.68E-02
Tubes cross section [m^2]	7.32E-03
Secondary fluid flow area, A_{ax} [m^2]	9.50E-03
Flow channel area [m^2]	1.15E-04
Flow channel perimeter [m]	2.49E-02
Hydraulic diameter, d_h [m]	0.02
Number of tubes in the bundle, N	37

calculated as:

$$v = \frac{G}{\rho A} \quad \text{(Eq. 2)}$$

At this point, the total reference mass per unit length, m_0 [kg/m], has been computed as the sum of the tube metal mass (m_t), the mass of fluid inside the tube (m_i) and the hydrodynamic mass (m_a), all expressed as mass per unit tube length, where:

$$m_t = \frac{\pi}{4}\left(d_o^2 - d_i^2\right)\rho_m$$
$$m_i = \frac{\pi}{4} d_i^2 \rho_i \quad \text{(Eq. 3)}$$
$$m_a = C_m \frac{\pi}{4} d_o^2 \rho$$

The virtual mass coefficient (i.e. the hydrodynamic mass coefficient)

Table 3
Input data for the selected sections.

	Secondary fluid inlet sect.	Recirculation sect.	Secondary fluid outlet sect.
Tube span, l [m]	0.928	0.890	0.88
Shellside fluid temperature, T [°C]	280.1	280.1	313.8
Tubeside fluid temperature, T_i [°C]	295	324.9	328.0
Tube outside surface boundary layer temperature, T_o [°C]	284.4	319.5	326.9
Section diameter, S_d [m]	0.059	0.038	0.059
Kinematic viscosity of the shellside fluid at T_o, ν' [m^2/s]	5.85E-07	7.377E-07	7.687E-07
Shellside fluid density, ρ [kg/m^3]	750.39	33.13	28.6
Tubeside fluid density, ρ_i [kg/m^3]	736.58	666.73	657.7

C_m can be estimated from Fig. 16.8.5 of the reference [12]. In this case, it has been assumed equal to 1.55. Hence, in the current evaluation, m_0 = 0.4518 kg/m.

Afterwards, the tube natural frequency (ω, rad/s) and the mode shape have been established. In particular, as in this section the tubes are connected to a tube sheet and to a baffle plate, they can be treated as a single span beam with fixed-pinned boundary conditions. Hence, the natural frequency for the first mode shape (i.e. for the most demanding) can be obtained as:

$$\omega = \frac{3.927^2}{l^2}\left(\frac{EI}{m_0}\right)^{1/2} \quad \text{(Eq. 4)}$$

A natural frequency of 4.572E+02 rad/s, corresponding to a cyclic frequency f of 72.76 s^{-1}, has been computed. Then, the logarithmic decrement coefficient δ, taking into account the damping phenomena, has been calculated on the basis of the Pettigrew theory explained in [12]. In particular, the Pettigrew's fractional damping coefficient ζ is given by:

$$\zeta = \frac{c_n d_0}{2m_0'\omega} \quad \text{(Eq. 5)}$$

where m'_0 is the reference mass per unit length calculated using $C_m = 1$, equal to 0.1178 in this case. Instead, as to the c_n coefficient, 0.00147 lb s/in^3 can be used for liquids whereas 0.00515 lb s/in^3 can be assumed for vapours and two-phase mixtures. The latter coefficient has been opportunely converted for the purpose of this assessment, and a value of 142.551 kg s/m^3 has been then obtained and adopted. With these assumptions, ζ = 2.101E-02 has been then calculated. Hence, the logarithmic decrement coefficient δ equal to 1.32E-01 s^2/m is obtained as:

$$\delta = 2\pi\zeta \quad \text{(Eq. 6)}$$

In order to perform the fluid elastic stability check, the parameter X, given by:

$$\mathrm{X} = \frac{m_0\delta}{\rho d_0^2} \quad \text{(Eq. 7)}$$

must be evaluated. For this case, it is equal to 8.28. Afterwards, the lower bound on critical flow velocity, indicated as v*, must be computed using the formulas available in Table 16.7.1 of reference [12] and depending on the layout arrangement and the range of X. Since v* is defined as:

$$v* = \frac{v_{crit}}{fd_0} \quad \text{(Eq. 8)}$$

For the present case, the v* velocity can be obtained from the formula:

$$v* = 2.8\mathrm{X}^{0.55} \quad \text{(Eq. 9)}$$

and the critical velocity is equal to 10.35 m/s. At this point, the usage factor for the fluid elastic stability check can be defined as the ratio between the critical velocity and cross-flow velocity, such as:

$$UF_{fs} = \frac{v_{crit}}{v} \quad \text{(Eq. 10)}$$

If the UF is greater than 1, the onset of vibration can be excluded. The higher is the UF, the higher is the probability that vibrations due to fluid elastic instabilities do not represent a concern. In the present case UF_{fs} = 0.99 is obtained, meaning that the onset of vibrations due to fluid-elastic instability cannot be excluded a priori.

Regarding the acoustic vibration check, necessary since in the assessed section the secondary fluid is in the state of saturated steam, the parameters reported in Table 4 have been considered.

First, the velocity of sound in the gas, c [m/s], of 600.5 m/s has been computed as:

$$c = \left(\frac{z\gamma R^*(T + 273.15)}{M}\right)^{0.5} \quad \text{(Eq. 11)}$$

Afterwards, the acoustic frequency f_a [1/s] of 1.430E+04 s^{-1} can be obtained as:

$$f_a = \frac{c}{2w} \quad \text{(Eq. 12)}$$

At this point, the Strouhal number S must be evaluated using figure 16.7.10 of the reference [12]. To this purpose, the lateral pitch of the tube bundle, p_l, has been defined, considering the tube layout angle of 60 °, as:

$$2p_l = p\frac{\sqrt{3}}{2} \quad \text{(Eq. 13)}$$

Table 4
Parameters for the acoustic vibration check.

Compressibility factor, z	1
Specific heat ratio, γ	1.33
Universal gas constant, R* [J / (kmol • K)]	8314.5
Molecular weight, M [kg/kmol]	18
Distance between the reflecting surface, w [m]	2.10E-02

and, consequently, the ratio p_l/d_0 equal to 0.606 can be computed. Therefore, a Strouhal number of 0.7 can be estimated and, consequently, the exciting frequency f_e [1/s] can be defined as

$$f_e = \frac{Sv}{d_0} \quad \text{(Eq. 14)}$$

In this case, f_e = 4.602E+02 s^{-1} is obtained. Lastly, the usage factor UF_{ac} can be defined as the ratio between the acoustic and the exciting frequency, such as:

$$UF_{ac} = \frac{f_a}{f_e} \quad \text{(Eq. 15)}$$

In the present case UF_{ac} = 31 is obtained, allowing excluding the onset of acoustic vibrations with a remarkable certainty.

Regarding the random excitation check, the effective random excitation coefficient, C_R*, is determined based on figure 16.7.6 of reference [12]. In this case, the value of 1.0E-02 has been considered. On this basis, the square root of the power-spectral-density of the excitation force per unit tube length, $S_p^{1/2}$, has been calculated equal to 0.247 using the formula:

$$S_p^{1/2} = \frac{1}{2}\rho v^2 d_0 C_R^* \quad \text{(Eq. 16)}$$

Afterwards, the mid-span root-mean-square amplitude of tube deflection, y_{rms}, can be calculated as:

$$y_{rms} = \frac{S_p^{1/2}}{\left(4\pi^5 f^3 m_0^2 \varsigma\right)^{1/2}} \quad \text{(Eq. 17)}$$

and, on its basis, the average tube vibration amplitude y can be found squaring the y_{rms} value. In this case, y = 3.02E-08 m is obtained. Assuming a very conservative safety factor equal to 0.2, the maximum allowable displacement can be found as:

$$y_{\lim} = 0.2(p - d_0) \quad \text{(Eq. 20)}$$

Then, the usage factor for the vibrations due to random excitation can be defined as the ratio between the maximum allowable displacement and the average tube displacement, as:

$$UF_{pf} = \frac{y_{\lim}}{y} \quad \text{(Eq. 21)}$$

Since in this case the computed usage factor is of the order of 104, the onset of vibrations due to random excitation can be definitely excluded. This outcome is confirmed also computing the tube pseudo-stress, σ* [Pa], which is the stress induced in the pipe by the deflection y. It is calculated by:

$$\sigma^* = \frac{24}{5}\frac{Ed_0 y}{l^2} \quad \text{(Eq. 18)}$$

Comparing it with the maximum allowable stress of the tube material (Table 1), a proper usage factor can be defined as:

$$UF_{stress} = \frac{S_m}{\sigma^*} \quad \text{(Eq. 19)}$$

Since in this case it is of the order of 10^5, the random excitation phenomena do not represent a concern neither from the stress point of view.

Lastly, the potential flow-induced vibrations due to parallel flow have been checked. To this purpose, considering the previously calculated secondary fluid flow area (Table 2), the axial flow velocity u_{ax} has been calculated as

$$u_{ax} = \frac{G}{\rho A_{ax}} \quad \text{(Eq. 24)}$$

In this case, u_{ax} = 5.177 m/s has been computed. Then, from figure 16.11.1 of reference [12], the dimensionless scale factors η_d, η_D and η_L

have been computed as function of the figures of merit fd_0/u_{ax}, fd_h/u_{ax} and f_l/u_{ax}, respectively. Moreover, from figure 16.11.2 of reference [12], the average disparity between theoretical and experimental displacement, C_R, has been obtained as function of the quantity dh/l. In Table 5 the obtained values have been reported.

At this point the mid-span root-mean-square amplitude of tube deflection, y_{rms}, can be computed as:

$$y_{rms} = C_R \eta_d \eta_D \eta_L \left[\frac{\rho d_0 \nu'^{0.5} N^{0.5}}{m_t f^{1.5} \varsigma^{1.5}} \right] u_{ax} \quad \text{(Eq. 25)}$$

and, on its basis, the average tube vibration amplitude y can be found squaring the y_{rms} value. In this case, y = 7.315E-05 m is obtained. Assuming a very conservative safety factor equal to 0.2, the maximum allowable displacement can be found as indicated in (Eq. 20) and the usage factor for the vibrations due to parallel flow check can be defined as shown in (Eq. 21). In the present case, $UF_{pf} = 17.4$ is obtained, allowing excluding the onset of vibrations due to parallel flow with a reasonable certainty. Therefore, it can be stated that with regard to the fluid elastic stability check within the secondary fluid outlet section minor problems seems to arise, in contrast to the checks concerning the parallel flow, random excitation and acoustic resonance, appearing verified. For this reason, it can be said that these phenomena do not seem to be significant.

Concerning the other two analysed sections, the details are not reported for brevity. It can be stated that the results of the flow-induced vibration assessment exhibit a very good response with regard to the secondary fluid inlet section, therefore vibration-induced issues can be ruled out. Instead, for the recirculation section, random excitation, parallel flow and acoustic resonance checks appear to be verified, in contrast to the fluid elastic stability one, where little problems emerge. In fact, the usage factor calculated for the fluid elastic stability check is slightly over unity within the recirculation region (Table 6). Therefore, for what was stated above, the check is verified although by a small margin.

Table 5
Figures of merit and dimensionless coefficients.

$f\,d_o/u_{ax}$	$f\,d_h/u_{ax}$	$f\,l/u_{ax}$	d_h/l	η_d	η_D	η_L	C_R
0.19	0.22	10.66	0.02	4.00	0.40	0.15	75.00

Table 6
Usage factors for the fluid elastic stability check calculated for the three analyzed sections.

Section	Usage Factor
Secondary fluid inlet	3.5
Recirculation	1.27
Secondary fluid outlet	0.99

5. Conclusions

Within the framework of the EUROfusion activities, a research campaign has been carried out at the University of Palermo in cooperation with ENEA Brasimone in order to investigate the structural performances of the STEAM facility by means of a pipe stress analysis, the 3D mechanical analysis of the OTSG mock-up and the preliminary study of the tube vibration within this component.

With regard to the performed pipe stress analysis, the STEAM surge line has been analysed and its original design has been improved in order to fulfil the structural design criteria while keeping displacements within acceptable values.

As to the 3D thermo-mechanical analysis of the OTSG mock-up, results show that, according to the considered standard, the structural integrity is ensured throughout most of the structure with exceptions in two critical areas requiring a more detailed study of the regions. Instead, in other critical areas, a revision of the contact modelling could help the structural performances response. Some solutions have been also proposed to overcome the emerged criticality.

Lastly, the flow-induced vibration assessment has been conducted within three different sections of the OTSG mock-up. The secondary fluid inlet section shows good results, instead, slight concerns arose from the study of the other two sections, but, for both, from the overall view of all the checks carried out, no big issues seem to emerge.

CRediT authorship contribution statement

I. Catanzaro: Writing – review & editing, Writing – original draft, Visualization, Validation, Resources, Methodology, Investigation, Formal analysis, Data curation, Conceptualization. **G. Bongiovì:** Writing – review & editing, Writing – original draft, Visualization, Validation, Resources, Methodology, Investigation, Formal analysis, Data curation, Conceptualization. **S. Giambrone:** Writing – review & editing, Writing – original draft, Visualization, Validation, Resources, Methodology, Investigation, Formal analysis, Data curation, Conceptualization. **A. Gioè:** Writing – review & editing, Writing – original draft, Visualization, Validation, Resources, Methodology, Investigation, Formal analysis, Data curation, Conceptualization. **P. Arena:** Writing – review & editing, Visualization, Validation, Methodology, Investigation, Data curation, Conceptualization. **A. Del Nevo:** Writing – review & editing, Visualization, Validation, Methodology, Investigation, Data curation, Conceptualization. **M. Eboli:** Writing – review & editing, Visualization, Validation, Methodology, Investigation, Data curation, Conceptualization. **S. Basile:** Writing – review & editing, Visualization, Validation, Methodology, Investigation, Data curation, Conceptualization. **R. Burlon:** Writing – review & editing, Visualization, Validation, Methodology, Investigation, Data curation, Conceptualization. **P. Chiovaro:** Writing – review & editing, Visualization, Validation, Methodology, Investigation, Data curation, Conceptualization. **P.A. Di Maio:** Writing – review & editing, Visualization, Validation, Supervision, Project administration, Methodology, Investigation, Funding acquisition, Data curation, Conceptualization. **M. Giardina:** Writing – review & editing, Visualization, Validation, Methodology, Investigation, Data curation, Conceptualization. **A. Quartararo:** Writing – review & editing, Visualization, Validation, Methodology, Investigation, Data curation, Conceptualization. **E. Tomarchio:** Writing – review & editing, Visualization, Validation, Methodology, Investigation, Data curation, Conceptualization. **E. Vallone:** Writing – review & editing, Visualization, Validation, Methodology, Investigation, Data curation, Conceptualization.

Declaration of competing interest

The authors declare that they have no known competing financial interests or personal relationships that could have appeared to influence the work reported in this paper.

Acknowledgement

This work has been carried out within the framework of the EUROfusion Consortium, funded by the European Union via the Euratom Research and Training Programme (Grant Agreement No 101052200 — EUROfusion). Views and opinions expressed are however those of the author(s) only and do not necessarily reflect those of the European Union or the European Commission. Neither the European Union nor the European Commission can be held responsible for them.

Data availability

No data was used for the research described in the article.

References

[1] P. Arena, et al., W-HYDRA: a new experimental platform for the water-cooled lead lithium breeding blanket, Nucl. Fusion 64 (2024) 076043, https://doi.org/10.1088/1741-4326/ad50e9.
[2] P. Arena, et al., Design and integration of the EU-DEMO water-cooled lead lithium breeding blanket, Energies. (Basel) 16 (4) (2023) 2069, https://doi.org/10.3390/en16042069.
[3] A. Vannoni, et al., The design of water loop facility for supporting the WCLL breeding blanket technology and safety, Energies. (Basel) 16 (23) (2023) 7746, https://doi.org/10.3390/en16237746.
[4] A. Tincani, et al., Conceptual design of the main ancillary systems of the ITER water cooled lithium lead test blanket system, Fusion Engineering and Design 167 (2021) 112345, https://doi.org/10.1016/j.fusengdes.2021.112345.
[5] ROHR2 v33, SIGMA Ingenieurgesellschaft mbH, Germany, www.rohr2.de.
[6] The American Society of Mechanical Engineers (ASME), Boiler and Pressure Vessel Code, Section III, Division 1 – Subsect. NC.
[7] P. Arena, "www.specialmetals.com catalogue", personal communication, 2023.
[8] RCC-MRx: Design and Construction Rules for Mechanical Components of Nuclear Installations, AFCEN, 2013.
[9] P. Lorusso, et al., Development of a Steam Generator Mock-Up for EU DEMO Fusion Reactor: Conceptual Design and Code Assessment, Energies. (Basel) 16 (2023) 3729, https://doi.org/10.3390/en16093729.
[10] ASME Boiler and Pressure Vessel Code, The American Society of Mechanical Engineering (ASME), 2015. Section II.
[11] ASME Boiler and Pressure Vessel Code, The American Society of Mechanical Engineering (ASME), 2015. Section VIII.
[12] K.P. SINGH, A.I. SOLER, Mechanical design of heat exchangers and pressure vessel components, First Edition, Springer-Verlag Berlin Heidelberg GmbH, 1984, https://doi.org/10.1007/978-3-662-12441-3. ISBN: 978-3-662-12443-7.
[13] M. Eboli, Review and new scaling of OTSG STEAM test section, 2023. https://idm.euro-fusion.org/?uid=2Q6BPE.